Dalton Transactions

Accepted Manuscript

This article can be cited before page numbers have been issued, to do this please use: T. Gao, R. Yan, A. J. Metherell, D. Cao, D. Ye and M. D. Ward, *Dalton Trans.*, 2017, DOI: 10.1039/C7DT03523C.

This is an Accepted Manuscript, which has been through the Royal Society of Chemistry peer review process and has been accepted for publication.

Accepted Manuscripts are published online shortly after acceptance, before technical editing, formatting and proof reading. Using this free service, authors can make their results available to the community, in citable form, before we publish the edited article. We will replace this Accepted Manuscript with the edited and formatted Advance Article as soon as it is available.

You can find more information about Accepted Manuscripts in the author guidelines.

Please note that technical editing may introduce minor changes to the text and/or graphics, which may alter content. The journal's standard Terms & Conditions and the ethical guidelines, outlined in our author and reviewer resource centre, still apply. In no event shall the Royal Society of Chemistry be held responsible for any errors or omissions in this Accepted Manuscript or any consequences arising from the use of any information it contains.

ROYAL SOCIETY OF CHEMISTRY

rsc.li/dalton

Cite this: DOI: 10.1039/c0xx00000x

www.rsc.org/xxxxxx

COMMUNICATION

Coordination mode-induced isomeric cyclometalated [Ir(tpy)(nbi)Cl](PF$_6$) complexes: distinct luminescence, self-assembly and cellular imaging behaviors†

Tai-Bao Gao,[a§] Run-Qi Yan,[b§] Alexander J. Metherell,[c] Deng-Ke Cao,[a]* De-Ju Ye[b]* and Michael D. Ward[c,d]*

Received (in XXX, XXX) Xth XXXXXXXXX 20XX, Accepted Xth XXXXXXXXX 20XX
DOI: 10.1039/b000000x

Two isomeric Ir(III) complexes Ir-O and Ir-R arising from the different coordination mode of a naphthalene-containing ligand, show distinct luminescence, self-assembly ability and cellular imaging behaviors.

Cyclometalated Ir(III) complexes possess many advantageous characteristics, such as good physicochemical stability, high photoluminescence quantum yields and facile color tuning,[1] which make them useful for a range of applications such as chemosensors,[2] phosphorescent emitters in organic light-emitting diodes (OLEDs),[3] cellular imaging,[4] information storage and security protection,[5] and catalysis.[6] Various Ir(III) complexes with different functional properties have been synthesized through incorporating one, two or three bidentate C^N cyclometalating ligands, thus forming [Ir(N^N^N)(C^N)X]$^+$,[7-9] Ir(C^N)$_2$(L^X),[10] or Ir(C^N)$_3$[11] complexes (where N^N^N = terpyridine (tpy) and its derivatives; C^N = cyclometalating ligands; X = anionic monodentate ligands; L^X = neutral/anionic bidentate ancillary ligands). Among these, complexes of the type [Ir(N^N^N)(C^N)X]$^+$ are of particular interest as the incorporation of tridentate N^N^N ligands (*e.g.* tpy) can dramatically enhance their chemical stability.[7a] Moreover, their luminescence and photo-catalyzing properties can be easily tuned by using different C^N ligands [*e.g.*, 2-phenyl-pyridine (ppyH) and its derivatives] and/or anionic monodentate ligands X (*e.g.*, Cl$^-$ and CN$^-$),[7] which facilitates their applications in photo-catalysis and cellular imaging.[7b,c,8] For example, Sato *et al*. first reported complex [Ir(tpy)(ppy)Cl](PF$_6$) (λ_{em} = 541 nm in CH$_3$CN), which served as an efficient photo-catalyst for CO$_2$ reduction with a quantum yield of 0.21.[8a] Inspired by this work, Bernhard's group later reported [Ir(tpy)(ppy)(CN)](PF$_6$),[7a] which showed a blue-shifted emission at 496 nm, indicating that different ligands X (Cl$^-$ *vs.* CN$^-$) can result in distinct emission wavelengths. They further found that the emission wavelengths and the photo-catalyzing ability of the [Ir(ttbutpy)(C^N)Cl](PF$_6$) complexes [Scheme S1, C^N = a series of fluorinated 5-methyl-2-phenylpyridine (mppy$^-$)] could be precisely optimized via using differently fluorinated mppy$^-$ ligands.[7b] Very recently, Long and Chao *et al.* synthesized three complexes [Ir(ttpy)(ppy)Cl](PF$_6$), [Ir(ttpy)(pq)Cl](PF$_6$) and [Ir(ttpy)(pbt)Cl](PF$_6$) for fluorescence imaging of mitochondrial dynamics in living cells (Scheme S2).[7c] They found that the C^N ligands ppy, pq and pbt with increasing π-electron conjugation could make the complexes emit at 551, 578 and 626 nm, respectively. So far, all reported [Ir(N^N^N)(C^N)X]$^+$ complexes have only incorporated benzene-based C^N ligands, such as ppy, pq and pbt (Scheme S2), which use their cyclometalating carbon atoms from benzene rings to coordinate with Ir(III) ions. There is still a lack of [Ir(N^N^N)(C^N)X]$^+$ complexes incorporating naphthalene-based C^N ligands. From the viewpoint of structure, a naphthalene-based C^N ligand could provide more cyclometalating carbon atoms (*e.g.*, C2 and C8 atoms in nbiH, Scheme 1) with respect to a benzene-based C^N ligand (*e.g.* 2-phenyl-pyridine). Moreover, the naphthalene-based C^N ligand could provide more π-electron conjugation, thus resulting in a cyclometalated Ir(III) complex with lower energy emission.[12]

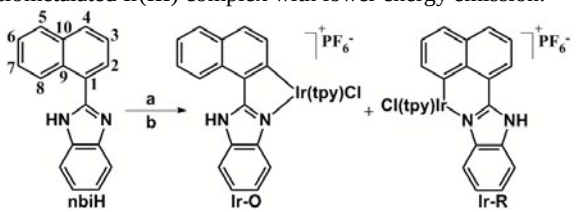

Scheme 1 Syntheses of complexes **Ir-O** and **Ir-R**. Reaction conditions: (a) Ir(tpy)Cl$_3$, EtOEtOH, 190 or 135 ^{o}C, 24 hours, Ar; (b) KPF$_6$.

In this paper, we reported a cyclometalating ligand 2-naphthalen-1-yl-1H-benzoimidazole (nbiH, Scheme 1), in which besides the imidazole nitrogen atom, the naphthalene unit is expected to coordinate with an Ir(III) ion through either of its carbon atoms C2 or C8. Thus, the ligand nbi$^-$ could chelate an Ir(III) ion in either a five- or six-membered ring chelating mode (Schemes 1 and S3). Based on nbiH coordinating in these two modes, we have obtained two isomeric [Ir(tpy)(nbi)Cl](PF$_6$) complexes, namely **Ir-O** and **Ir-R**. To the best of our knowledge, these are the first examples of a matched pair of isomeric [Ir(N^N^N)(C^N)X]$^+$ complexes. Herein, we discuss their syntheses, and the significant differences in luminescence, self-assembly and cellular imaging behaviors arising from their different structures.

As shown in Scheme 1, complexes **Ir-O** and **Ir-R** were

View Article Online
DOI: 10.1039/C7DT03523C

synthesized together through the reaction of nbiH and $Ir(tpy)Cl_3$ at 190 ºC or 135 ºC for 24 hours, followed by the anion exchange of Cl^- with PF_6^- (see ESI for synthesis details). Their mixture was purified by silica column chromatography, sequentially obtaining **Ir-O** and **Ir-R** in 24% and 43% yields, respectively, for the reaction temperature of 190 ºC, and in 19% and 47% yields, respectively, for 135 ºC. This indicates that reaction temperature can influence the yields of two complexes. However, it is not clear why the yield of **Ir-R** is always higher that of **Ir-O**, although the molecular structure of **Ir-R** is more hindered or strained than that of **Ir-O**. Their chemical structures were characterized by ^{1}H NMR, IR, ESI-MS and elemental analysis (see ESI), revealing the formation of isomeric complexes $[Ir(tpy)(nbi)Cl](PF_6)$. To further clarify the structures of **Ir-O** and **Ir-R**, the single crystals of **Ir-O**·Et_2O·CH_3COCH_3 and **Ir-R** were grown from an acetone/diethyl ether and $CHCl_3/CH_3OH$ respectively, and measured by X-ray crystallography. Their crystallographic data are shown in Table S2, and the selected bond distances and bond angles are listed in Tables S3 and S4.

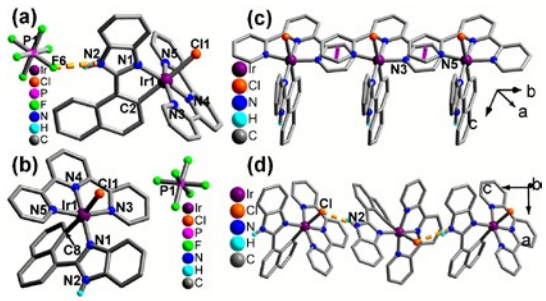

Fig. 1 Molecular structures of **Ir-O** (a) and **Ir-R** (b), and supramolecular chains in **Ir-O** (c) and **Ir-R** (d) (yellow and magenta dot lines showing hydrogen bonds and π···π stacking interactions, respectively).

As shown in Fig. 1a, the Ir(III) ion in **Ir-O** shows a distorted octahedral coordination geometry. Four of the six coordination sites are occupied by one Cl^- ion, and three nitrogen atoms (N3, N4 and N5) from the tpy ligand. The remaining two coordination sites are filled with atoms C2 and N1 from the ligand nbi^-. Around the Ir(III) ion, atom C2 is at the *trans* position of Cl^- (Fig. 1a). The molecular structure of **Ir-R** is clearly different from that of **Ir-O**, in which an Ir(III) ion is coordinated by atom C8 instead of atom C2 from the ligand nbi^- (Fig. 1b). The Ir-Cl bonds in both **Ir-O** [2.447(4) Å] and **Ir-R** [2.4638(13) Å] are longer than those in $Ir(tpy)Cl_3$ [2.347-2.370 Å],[13] due to the strong σ donating ability of the Ir-C2/C8 bond.[14] The Ir-N4 bonds in both **Ir-O** [1.959(12) Å] and **Ir-R** [1.960(4) Å] are significantly shorter than the other Ir-N bonds [2.047(12)-2.063(4) Å], which is attributed to geometric constraints arising from the tridentate binding of tpy.[15]

Complexes **Ir-O** and **Ir-R** are isomeric owing to the different coordination modes of their nbi^- ligands. As shown in Figs. 1a and 1b, the nbi^- ligand in **Ir-O** chelates an Ir(III) ion through a five-membered ring chelating mode, while a six-membered chelate ring occurs in **Ir-R**. This difference in coordination mode results in a significantly different extent of twist within the nbi^- ligand between **Ir-O** and **Ir-R**. All ten C atoms belonging to a naphthalene unit in **Ir-O** are at the same plane (Fig. S11 top). In contrast, the naphthalene unit in **Ir-R** shows a significant twist (Fig. S11 bottom), with a 14.2(1)º dihedral angle between the plane defined by atoms C5-C7 and the plane defined by C1-C4 and C9 and C10 atoms. In addition, the dihedral angle between benzoimidazole unit and benzene ring containing C1 atom (Fig. S11) in **Ir-R** is 29.0(1)º, which is significantly larger than that in **Ir-O** [10.2(1)º]. Five-membered chelate ring, like that seen for ligand nbi^- in **Ir-O**, are often observed in Ir(III) complexes incorporating naphthalene-based C^N ligands (Scheme S4).[16-21] However, the six-membered chelate ring seen in **Ir-R** is quite unusual, and has not been reported so far for a naphthalene-based C^N ligand.

Complexes **Ir-O** and **Ir-R** possess dramatically different supramolecular interactions. First, the $[Ir(tpy)(nbi)Cl]^+$ cation and its counter anion PF_6^- in **Ir-O** show a hydrogen-bonding interaction between them [N2-H···F6 = 2.897(1) Å][22] (Fig. 1a), while no such hydrogen-bonding interaction occurs in **Ir-R** (Fig. 1b). Second, both **Ir-O** and **Ir-R** reveal supramolecular chain structure (Figs. 1c and 1d). Neighboring $[Ir(tpy)(nbi)Cl]^+$ cations in this chain are associated through π···π stacking interactions between two pyridine rings of tpy ligands from adjacent $[Ir(tpy)(nbi)Cl]^+$ units [plane–plane distance: 3.37 Å][23] in **Ir-O**, whereas there a weak hydrogen bond [N2-H···Cl^a = 3.206(1) Å, symmetry code a = -x + 3/2, y, z + 1/2][22] in **Ir-R**.

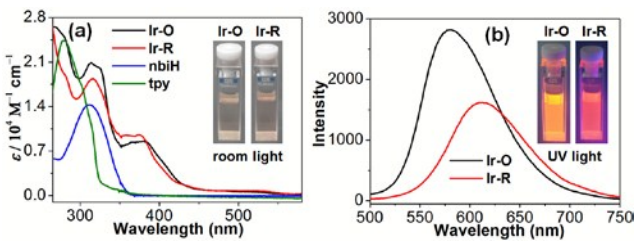

Fig. 2 (a) UV-vis absorption spectra and (b) luminescence spectra of **Ir-O**, **Ir-R**, nbiH and tpy in CH_3CN (λ_{ex} = 398 nm). Inset: the photographs under room light or 365 nm light.

Ir-O and **Ir-R** have different optical spectroscopic properties. Their UV-vis spectra in CH_3CN at room temperature are in Fig. 2a and Table S5. The high-energy absorption bands in **Ir-O** appear at 269, 314 and 325 nm, while at 280 and 316 nm in **Ir-R**. These absorption bands can be assigned to spin-allowed ligand-centered (^{1}LC) transitions (nbi^- and tpy ligands), which are comparable to the $\pi\rightarrow\pi^*$ absorption bands of nbiH (312 nm) and tpy (279 nm). The low-energy broad absorption band of **Ir-O** (maximum at 384 nm) reveals a slight red shift compared to that of **Ir-R** (maximum at 376 nm), probably due to the fact that the nbi^- ligand in **Ir-O** less twisted and therefore has better π-conjugation (Fig. S11) than that in **Ir-R**. These low-energy absorption bands in two complexes are mainly attributed to spin-allowed metal-to-ligand charge transfer (^{1}MLCT) because the isolated ligands nbiH and tpy have no obvious absorption around 380 nm. The weaker absorption tails towards 570 for **Ir-O** and **Ir-R** correspond to ^{3}MLCT absorption.[9a,24] The UV-vis spectra of **Ir-O** and **Ir-R** were also measured in phosphate buffer solution (PBS, pH = 7.4, 10% DMSO) (Fig. S14, Table S5), showing an increase in MLCT absorption intensity at ~450 nm probably due

View Article Online
DOI: 10.1039/C7DT03523C

to the increasing solvent polarity from CH_3CN to PBS.

Complexes **Ir-O** and **Ir-R** show different luminescence properties in CH_3CN at room temperature (Fig. 2b, Table S5). Compared to **Ir-O** with a strong emission at 581 nm, complex **Ir-R** displays a weaker and red-shifted emission at 612 nm (Fig. 2b). This could be due to the fact that the six-membered chelate ring in **Ir-R**, and the resultant substantial twist of the nbi$^-$ ligand might not only destabilize the highest occupied molecular orbitals (HOMOs), but also promote additional non-radiative processes. The luminescence quantum yields (Φ) and lifetimes (τ) of **Ir-O** in air equilibrated CH_3CN were found to be ~2.1%, and 165 ns (93%) and 296 ns (7%), which are both significantly larger compared to **Ir-R** [Φ = 0.56% and τ = 86 ns (91%) and 169 ns (9%)]. Such dual-exponential decay for **Ir-O** and **Ir-R** could be attributed to molecular aggregation in solution through π···π stacking interactions and/or hydrogen interactions (see experiments below).[25] The broad and unstructured emissions of **Ir-O** and **Ir-R** indicate that their emissive excited states have predominantly ^{3}MLCT character. This was confirmed by their luminescence spectra measured at 77 K,[10b] exhibiting clearly blue-shifted emissions at 552, 599 and 655 nm for **Ir-O**, and 581 and 633 nm for **Ir-R** (Fig. S15, Table S5). The luminescence spectra of **Ir-O** and **Ir-R** were further measured in PBS (pH = 7.4, 10% DMSO) at room temperature (Fig. S16). The two complexes exhibited broad emission bands, 580 nm for **Ir-O** and 610 nm for **Ir-R**, which are comparable to their emission bands in CH_3CN (581 nad 612 nm, respectively), indicating that the solvents (CH_3CN and PBS) only slightly influence their excited state energies. Moreover, both **Ir-O** and **Ir-R** in CH_3CN showed acid/base-induced luminescence switch between on state and off state. Upon addition of tetrabutylammonium hydroxide (TBAOH) (Figs. S17 and S18), both complexes revealed gradual decrease in luminescence intensity due to the deprotonation of the imidazole units in their nbi$^-$ ligands (*i.e.* the formation of neutral species). Both **Ir-O** and **Ir-R** recovered their original luminescent states after adding some TFA to neutralize the involved TBAOH (Figs. S19 and S20).

We subsequently compared the self-assembly ability of **Ir-O** and **Ir-R** in PBS buffer. Dynamic light scattering (DLS) analysis showed that **Ir-O** (20 μM) could easily self-assemble into monodispersed nanoparticles, with a mean hydrodynamic diameter of ~ 100 nm (Fig. S21). This was also confirmed by transmission electron microscopy (TEM) analysis, showing spherical nanoparticles with an average size of ~90 nm (Fig. S21). In contrast, there were no nanoparticles observed for **Ir-R** under the same conditions. This difference in aggregation properties in solution can be correlated with the differences in crystal packing between **Ir-O** and **Ir-R**. Complex **Ir-O** possesses strong intermolecular π···π stacking interactions as revealed by its crystal structure (Fig. 1c), in which the molecules are orderly packed into superstructures, facilitating the self-assembling into nanoparticles. However, **Ir-R** possesses a more twisted structure and lacks intermolecular π···π stacking interactions in the crystalline state (Fig. 1d), and shows no evidence for formation of nanoparticles in solution. As such, **Ir-R** can be easily dissolved in PBS buffer to form a clear solution. This was also reflected in the much smaller oil-water partition coefficient (logP, -0.717) of **Ir-R** compared to **Ir-O** (-0.220) (Table S6). These results revealed that different coordination modes of ligands nbi$^-$ between **Ir-O** and **Ir-R** could cause distinct intermolecular interactions, thus resulting in different photophysical properties in solution.

To evaluate the properties of **Ir-O** and **Ir-R** in cellular imaging, we first tested their cytotoxicity against human cervical cancer HeLa cells using 3-(4,5-dimethylthiazol-2-yl)-2,5-diphenyltetrazolium bromide (MTT) assay. No adverse effect towards HeLa cells was observed when incubated with 20 μM **Ir-O** or **Ir-R** for 24 hours (Fig. S22), demonstrating that both complexes had good biocompatibility for the cellular imaging applications. We then incubated HeLa cells with either 20 μM **Ir-O** or **Ir-R** for different times (0, 1, 3, and 6 h), and the luminescence images were acquired using a Confocal laser scanning microscopy (CLSM). Our experiment results showed that both **Ir-O** and **Ir-R** could enter into HeLa cells and generate time-dependent enhanced intracellular luminescence (Fig. S23). After incubation for 3 h, the luminescence in HeLa cells stained with **Ir-O** was brighter than that with **Ir-R**, presumably owing to the higher luminescence quantum yield of **Ir-O** compared to **Ir-R** (Table S5). In addition, the enhanced lipophilicity might also enhance its uptake into HeLa cells, contributing to the higher intracellular luminescence in cells relative to **Ir-R**. These results suggested that complex **Ir-O** is more appropriate for cellular imaging studies compared to **Ir-R**. To further elucidate the intracellular locations of **Ir-O**, HeLa cells were incubated with **Ir-O** (20 μM) for 3 hours, and then co-stained with lysosomal tracker (Lyso Tracker Green DND-26). As shown in Fig. 3, HeLa cells incubated with **Ir-O** showed bright intracellular luminescence (pseudo red color), which overlaid very well with the green fluorescence from the lyso tracker, implying that **Ir-O** localized mainly in the lysosomes of HeLa cells. These results indicated that **Ir-O** had a high capacity to accumulate and stain the lysosomes of live cells, which was also revealed in certain cyclometalated Ir(III) complexes.[26]

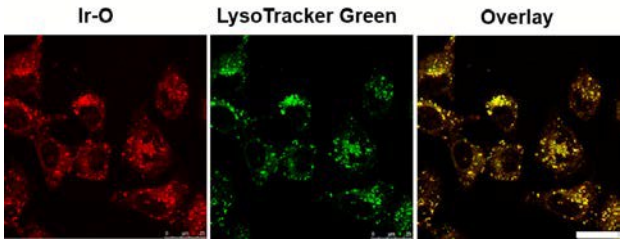

Fig. 3 Confocal laser scanning microscopy images of Hela cells stained with **Ir-O** (20 μM, λ_{ex} = 405 nm, pseudo red color) (left), and Lyso Tracker Green DND-26 (1 μM, λ_{ex} = 514 nm, pseudo green color). Scale bar: 25 μm.

In conclusion, two isomeric [Ir(tpy)(nbi)Cl](PF$_6$) complexes, **Ir-O** and **Ir-R**, have been synthesized using the ambidentate naphthalene-based C^N ligand nbiH (Scheme 1). Their crystal structures indicate that an {Ir(tpy)Cl}$^{2+}$ unit is chelated by a nbi$^-$ ligand using a carbon atom from naphthalene unit and an imidazole nitrogen atom (atoms C2 and N1 in **Ir-O**, and atoms C8 and N1 in **Ir-R**, Fig. 1a and 1b). Thus, complexes **Ir-O** and **Ir-R** are isomeric, which contain five- and six-membered chelate rings, respectively. The nbi$^-$ ligand in **Ir-R** shows significant torsional distortion, which is confirmed by the non-coplanarity of all ten C atoms belonging to its naphthalene unit, and the large dihedral angle between benzoimidazole unit and naphthalene unit.

View Article Online
DOI: 10.1039/C7DT03523C

The structural differences between **Ir-O** and **Ir-R** result in significantly different physiochemical properties and ability to aggregate to nanoparticles in solution. Of the two complexes, **Ir-O** is more appropriate for cell imaging, showing a high capacity to accumulate and stain the lysosomes of live cells, which could be assigned to its relatively high luminescence quantum yield and molecular self-assembly behavior. Complexes **Ir-O** and **Ir-R** are the first pair of coordination mode-induced isomers among naphthalene-based cyclometalated Ir(III) complexes. In further work, we will explore the possibility of using this approach to construct the others isomeric cyclometalated Ir(III) complexes, for example $[Ir(C^N)_2(C^N')]$ complexes.

This work was supported by the National Natural Science Foundation (NSF) of China (21505070 and 21632008), the NSF of Jiangsu Province, China (BK 20141314).

Notes and references

[a]*State Key Laboratory of Coordination Chemistry, School of Chemistry and Chemical Engineering, Nanjing University, Nanjing 210093, P. R. China.*
[b]*State Key Laboratory of Analytical Chemistry for Life Science, School of Chemistry and Chemical Engineering, Nanjing University, Nanjing 210093, P. R. China.*
[c]*Department of Chemistry, University of Sheffield, Sheffield S3 7HF, UK.*
[d]*Department of Chemistry, University of Warwick, Coventry CV4 7AL, UK.*
Corresponding authors: dkcao@nju.edu.cn; dejuye@nju.edu.cn; M.D.Ward@warwick.ac.uk.
Author contributions:[§]*These authors contributed equally.*

†Electronic Supplementary Information (ESI) available: Physical measurements, synthesis, crystallographic data, and some figures including ^{1}H NMR spectra, XRD pattern, structure, luminescence spectra, TEM images and cellular imaging behaviors.

1 (*a*) Y. You and S. Y. Park, *Dalton Trans.*, 2009, 1267.
2 (*a*) M. Wang, K.-H. Leung, S. Lin, D. S.-H. Chan, D. W. J. Kwong, C.-H. Leung and D.-L. Ma, *Sci. Rep.*, 2014, **4**, 6794; (*b*) K. Y. Zhang, J. Zhang, Y. Liu, S. Liu, P. Zhang, Q. Zhao, Y. Tang and W. Huang, *Chem. Sci.*, 2015, **6**, 301.
3. (*a*) D. Xia, B. Wang, B. Chen, S. Wang, B. Zhang and J. Ding, *Angew. Chem., Int. Ed.*, 2014, **53**, 1048; (*b*) T. Giridhar, C. Saravanan, W. Cho, Y. G. Park, J. Y. Lee and S.-H. Jin, *Chem. Commun.*, 2014, **50**, 4000; (*c*) P. Tao, W.-L. Li, J. Zhang, S. Guo, Q. Zhao, H. Wang, B. Wei, S.-J. Liu, X.-H. Zhou, Q. Yu, B.-S. Xu and W. Huang, *Adv. Funct. Mater.*, 2016, **26**, 881.
4 (*a*) E. Baggaley, J. A. Weinstein and J. A. G. Williams, *Coord. Chem. Rev.*, 2012, **256**, 1762; (*b*) (*b*) K. K.-W. Lo and K. Y. Zhang, *RSC Adv.*, 2012, **2**, 12069.
5 H. Sun, S. Liu, W. Lin, K. Y. Zhang, W. Lv, X. Huang, F. Huo, H. Yang, G. Jenkins, Q. Zhao and W. Huang, *Nat. Commun.*, 2014, **5**, 4601.
6 (*a*) J.-G. Cai, Z.-T. Yu, Y.-J. Yuan, F. Li and Z.-G. Zou, *ACS Catal.*, 2014, **4**, 1953; (*b*) C. Yang, F. Mehmood, T. L. Lam, S. L.-F. Chan, Y. Wu, C.-S. Yeung, X. Guan, K. Li, C. Y.-S. Chung, C.- Y. Zhou, T. Zou and C.-M. Che, *Chem. Sci.*, 2016, **7**, 3123 and references therein.
7 (*a*) D. N. Chirdon, W. J. Transue, H. N. Kagalwala, A. Kaur, A. B. Maurer, T. Pintauer and S. Bernhard, *Inorg. Chem.*, 2014, **53**, 1487; (*b*) J. A. Porras, I. N. Mills, W. J. Transue and S. Bernhard, *J. Am. Chem. Soc.*, 2016, **138**, 9460. (*c*) H. Huang, L. Yang, P. Zhang, K. Qiu, J. Huang, Y. Chen, J. Diao, J. Liu, L. Ji, J. Long, H. Chao, *Biomaterials*, 2016, **83**, 321.
8 (*a*) S. Sato, T. Morikawa, T. Kajino and Osamu Ishitani, *Angew. Chem., Int. Ed.*, 2013, **52**, 988; (*b*) K. Garg,Y. Matsubara, M. Z. Ertem, A. Lewandowska-Andralojc, S. Sato, D. J. Szalda, J. T. Muckerman and E. Fujita, *Angew. Chem., Int. Ed.*, 2015, **54**, 14128.
9 (*a*) R. O. Reithmeier, S. Meister, B. Rieger, A. Siebel, M. Tschurl, U. Heiz and E. Herdtweck, *Dalton Trans.*, 2014, **43**, 13259; (*b*) R. O. Reithmeier, S. Meister, A. Siebel and B. Rieger, *Dalton Trans.*, 2015, **44**, 6466.
10 T. Hu, L. He, L. Duan and Y. Qiu, *J. Mater. Chem.*, 2012, **22**, 4206; (b) (*b*) S. Ladouceur and E. Zysman-Colman, *Eur. J. Inorg. Chem.*, 2013, 2985.
11 (*a*) K. A. McGee and K. R. Mann, *Inorg. Chem.*, 2007, **46**, 7800; (*b*) Y. Zheng, A. S. Batsanov, R. M. Edkins, A. Beeby and M. R. Bryce, *Inorg. Chem.*, 2012, **51**, 290.
12 W.-S. Huang, J. T. Lin, C.-H. Chien, Y.-T. Tao, S.-S. Sun and Y.-S. Wen, *Chem. Mater.*, 2004, **16**, 2480.
13 M. Dobroschke, Y. Geldmacher, I. Ott, M. Harlos, L. Kater, L. Wagner, R. Gust, W. S. Sheldrick, A. Prokop, *ChemMedChem*, 2009, **4**, 177.
14 S. Obara, M. Itabashi, F. Okuda, S. Tamaki, Y. Tanabe, Y. Ishii, K. Nozaki and M. Haga, *Inorg. Chem.*, 2006, **45**, 8907.
15 A. J. Wilkinson, H. Puschmann, J. A. K. Howard, C. E. Foster and J. A. G. Williams, *Inorg. Chem.*, 2006, **45**, 8685.
16 S. A. Denisov, Y. Cudre, P. Verwilst, G. Jonusauskas, M. Marin-Suarez, J. F. Fernandez-Sanchez, E. Baranoff, and N. D. McClenaghan, *Inorg. Chem.*, 2014, 53, 2677.
17 Q. Zhao, C.-Y. Jiang, M. Shi, F.-Y. Li, T. Yi, Y. Cao and C.-H. Huang, *Organometallics*, 2006, **25**, 3631.
18 (*a*) T. Yu, Y. Niu, S. Yu, Z. Xu, Y. Zhao, H. Zhang, *J. Organometallic Chem.*, 2017, **830**, 85; (*b*) S. P.-Y. Li, A. M.-H. Yip, H.-W. Liu, K. K.-W. Lo, *Biomaterials*, 2016, **103**, 305.
19 S. Takizawa, J. Nishida, T. Tsuzuki, S. Tokito and Y. Yamashita, *Inorg. Chem.*, 2007, **46**, 4308.
20 X. Xu, Y. Zhao, J. Dang, X. Yang, G. Zhou, D. Ma, L. Wang, W.-Y. Wong, Z. Wu and X. Zhao, *Eur. J. Inorg. Chem.*, 2012, 2278.
21 S.-F. Huang, H.-Z. Sun, Guo-Gang Shan, F.-S. Li, Q.-Y. Zeng, K.-Y. Zhao and Z.-M. Su, *Dyes and Pigments*, 2017, **139**, 524.
22 S.-Z. Hu, Z.-X. Xie and C.-H. Zhou, *Acta Phys. -Chim. Sin.*, 2010, **26**, 1795.
23 C. Janiak, *J. Chem. Soc., Dalton Trans.*, 2000, 3885.
24 (*a*) M. Mydlak, C. Bizzarri, D. Hartmann, W. Sarfert, G. Schmid and L. D. Cola, *Adv. Funct. Mater.*, 2010, **20**, 1812; (*b*) Y. You, S. Lee, T. Kim, K. Ohkubo, W.-S. Chae, S. Fukuzumi, G.-J. Jhon, W. Nam and S. J. Lippard, *J. Am. Chem. Soc.*, 2011, **133**, 18328.
25 D.-K. Cao, J.-S. Hu, M.-Q. Li, D.-P. Gong, X.-X. Li and M. D. Ward, *Dalton Trans.*, 2015, **44**, 21008 and references therein.
26 (*a*) S. Moromizato, Y. Hisamatsu, T. Suzuki, Y. Matsuo, Ryo Abe and S. Aoki, *Inorg. Chem.*, 2012, **51**, 12697; (b) L. He, Y. Li, C.-P. Tan, R.-R. Ye, M.-H. Chen, J.-J. Cao, L.-N. Ji and Z.-W. Mao, *Chem. Sci.*, 2015, **6**, 5409.

View Article Online
DOI: 10.1039/C7DT03523C

TOC

Two isomeric Ir(III) complexes **Ir-O** and **Ir-R** arising from the different coordination mode of a naphthalene-containing ligand, show distinct luminescence, self-assembly ability and cellular imaging behaviors.